



Supplement of

On the contribution of fast and slow responses to precipitation changes caused by aerosol perturbations

Shipeng Zhang et al.

Correspondence to: Shipeng Zhang (shipeng.zhang@physics.ox.ac.uk)

The copyright of individual parts of the supplement might differ from the article licence.

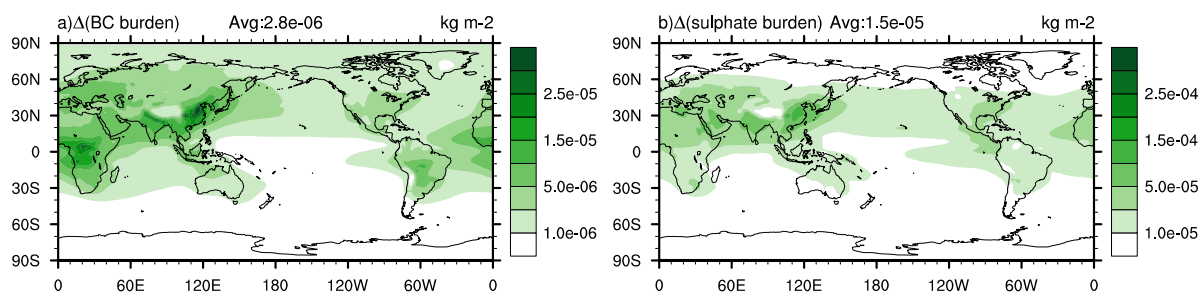


Figure S1. ECHAM6-HAM2 simulated global distribution of (a) BC burden (vertical-integrated aerosol mass) difference between 10BC case and baseline, (b) sulphate burden difference between 5SUL case and baseline

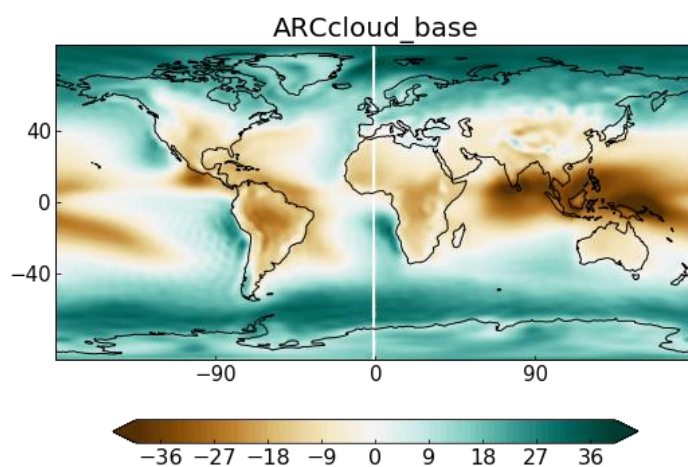


Figure S2. ECHAM6-HAM2 simulated global distribution of atmospheric radiative cooling from clouds. Unit: W/m²

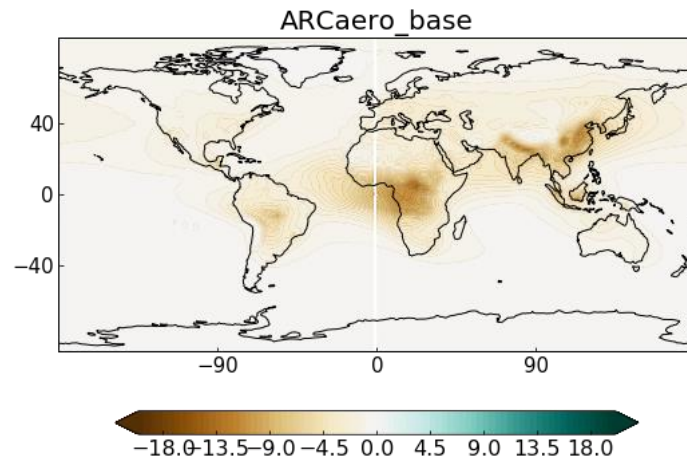


Figure S3. ECHAM6-HAM2 simulated global distribution of atmospheric radiative cooling from aerosols. Unit: W/m²

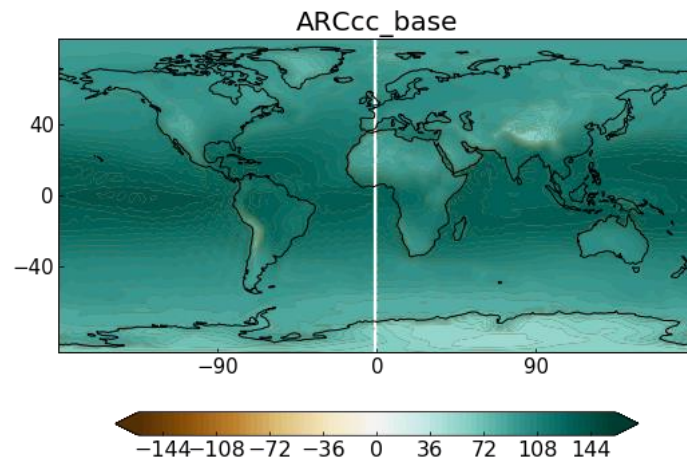


Figure S4. ECHAM6-HAM2 simulated global distribution of atmospheric radiative cooling from clear-clean sky. Unit: W/m²

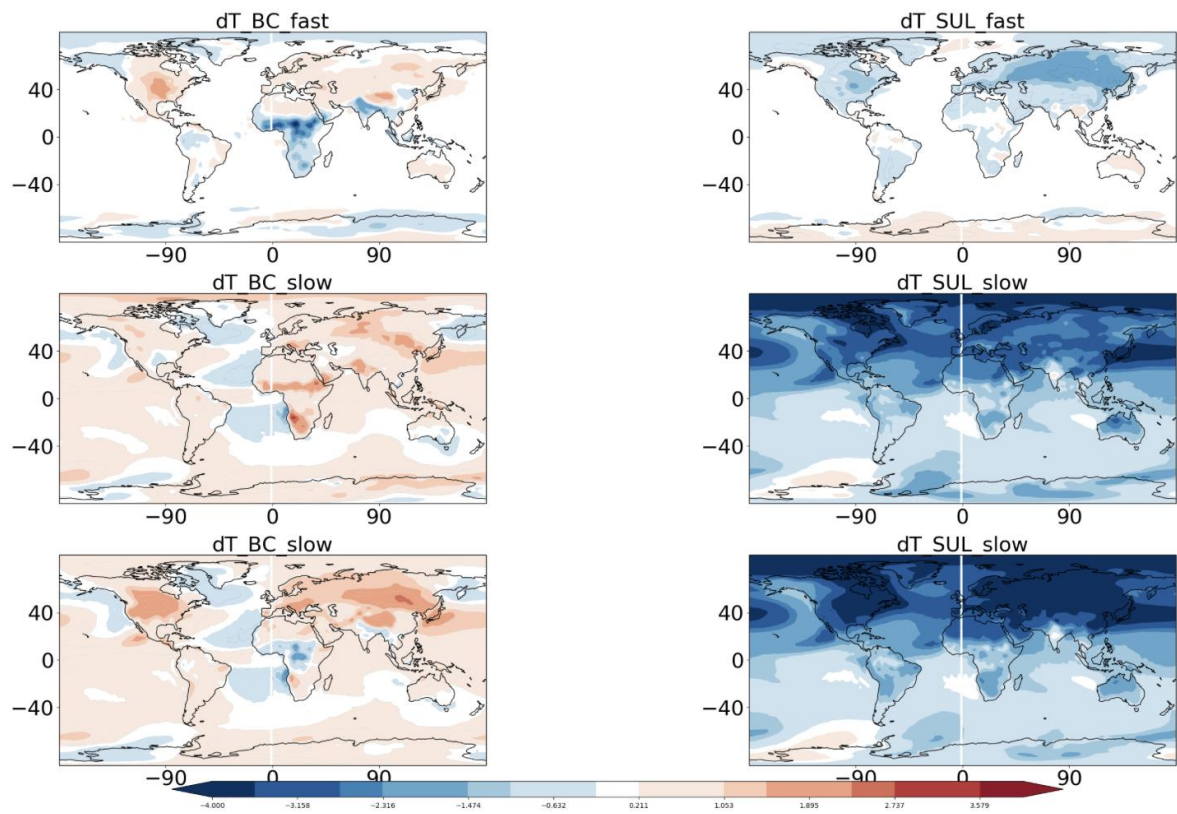


Figure S5. ECHAM6-HAM2 simulated geographical patterns of multi-annual mean surface temperature change in response to increasing (left column) 10 times BC emission and (right column) 5 times SUL precursor emission for (first row) total, (second row) fast, and (third row) slow responses.

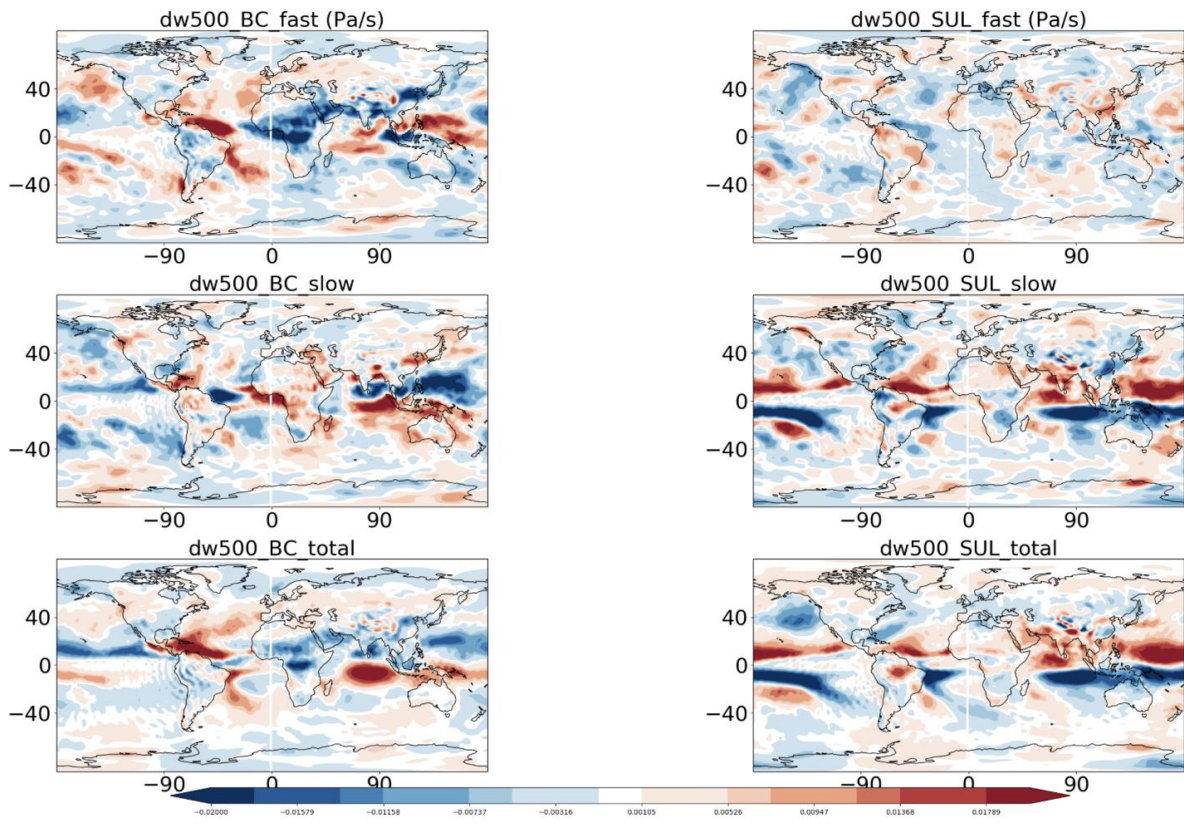


Figure S6. ECHAM6-HAM2 simulated geographical patterns of multi-annual mean vertical pressure velocity change in response to increasing (left column) 10 times BC emission and (right column) 5 times SUL precursor emission for (first row) total, (second row) fast, and (third row) slow responses.

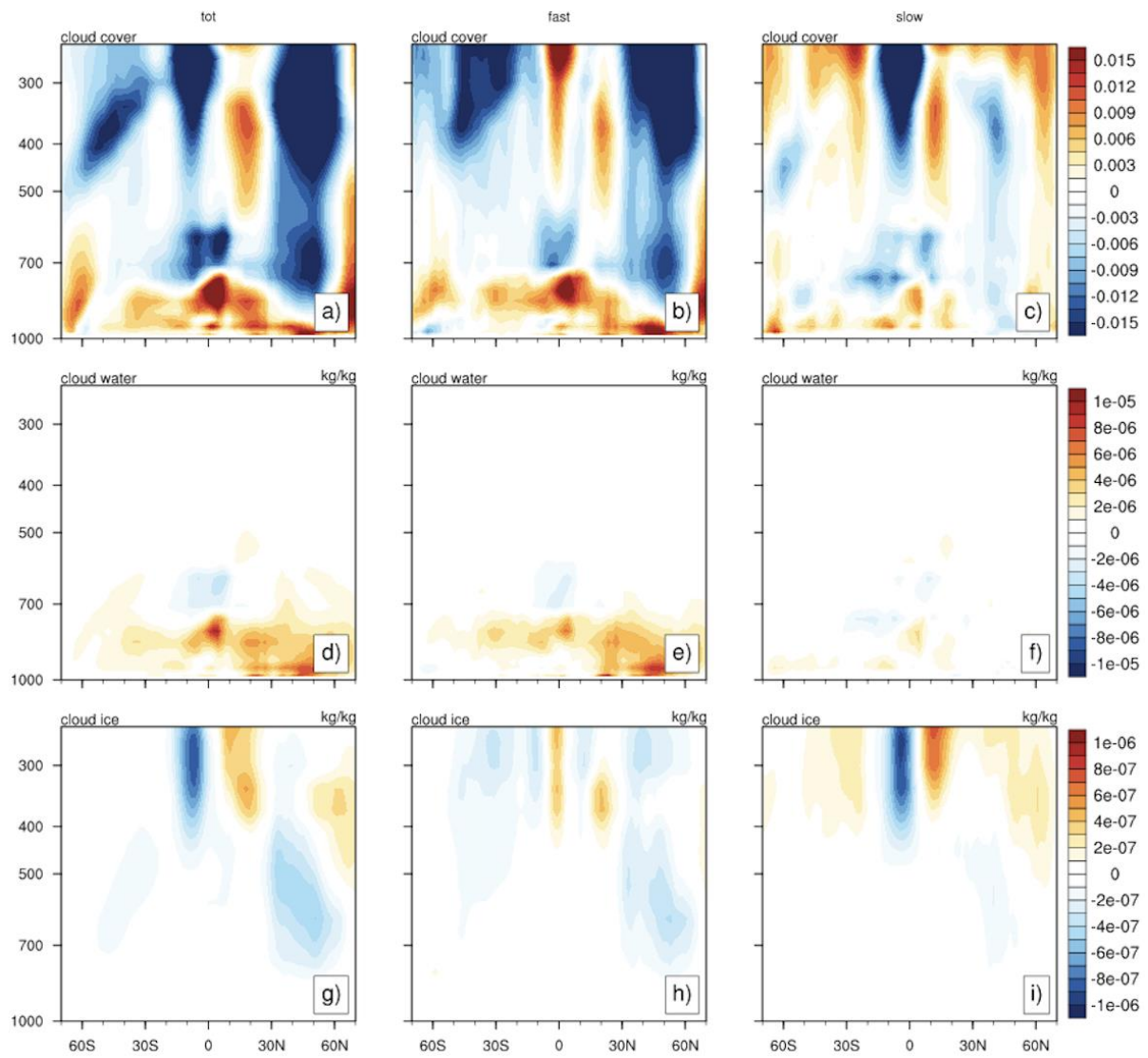


Figure S7. ECHAM6-HAM2 simulated multi-annual (left column) total, (middle column) fast, and (right column) slow responses of zonally averaged (a, b, c) cloud cover, (d, e, f) cloud water, and (g, h, i) cloud ice in response to 10 times BC emission.

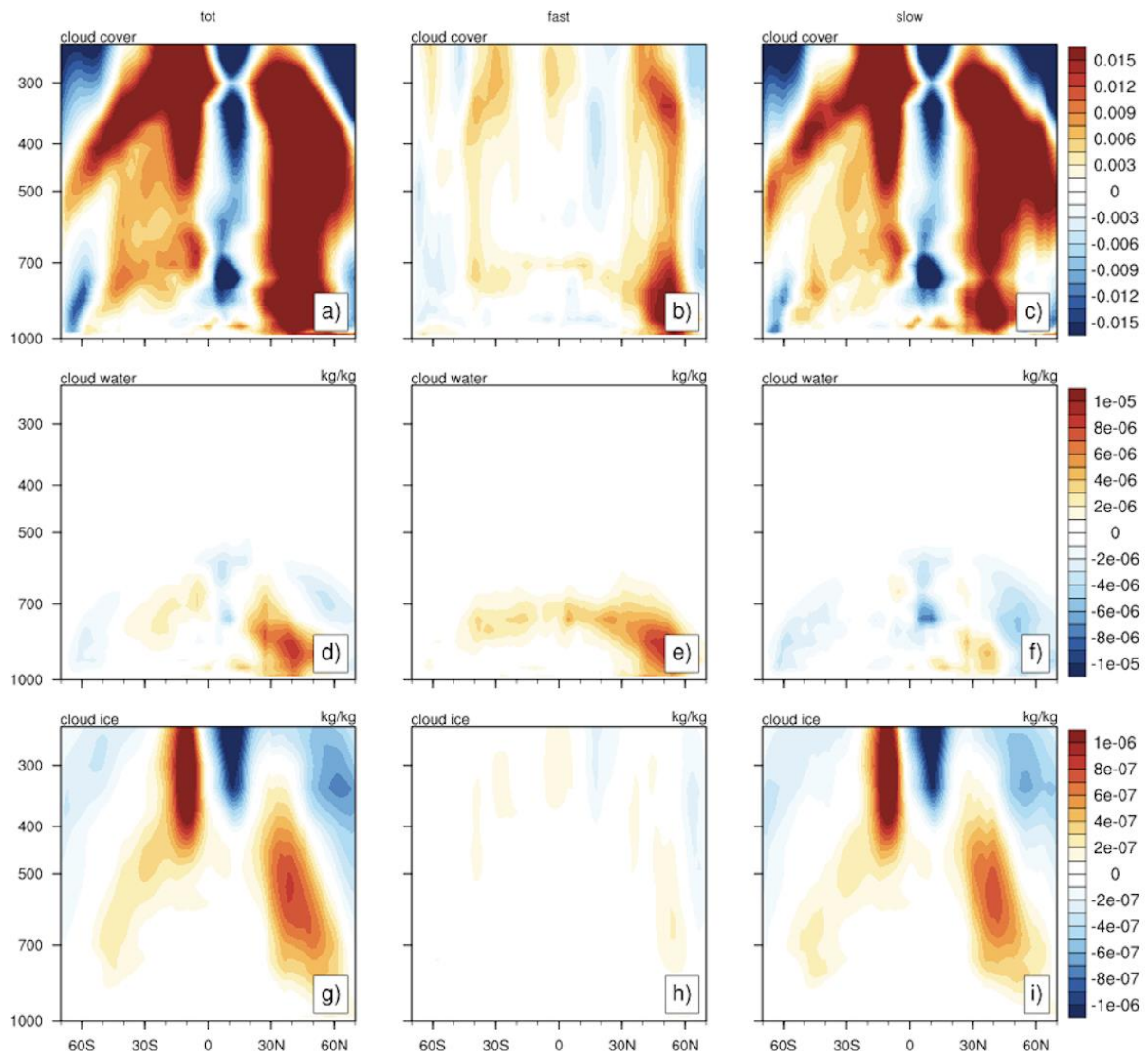


Figure S8. ECHAM6-HAM2 simulated multi-annual (left column) total, (middle column) fast, and (right column) slow responses of zonally averaged (a, b, c) cloud cover, (d, e, f) cloud water, and (g, h, i) cloud ice in response to 5 times SUL emission.

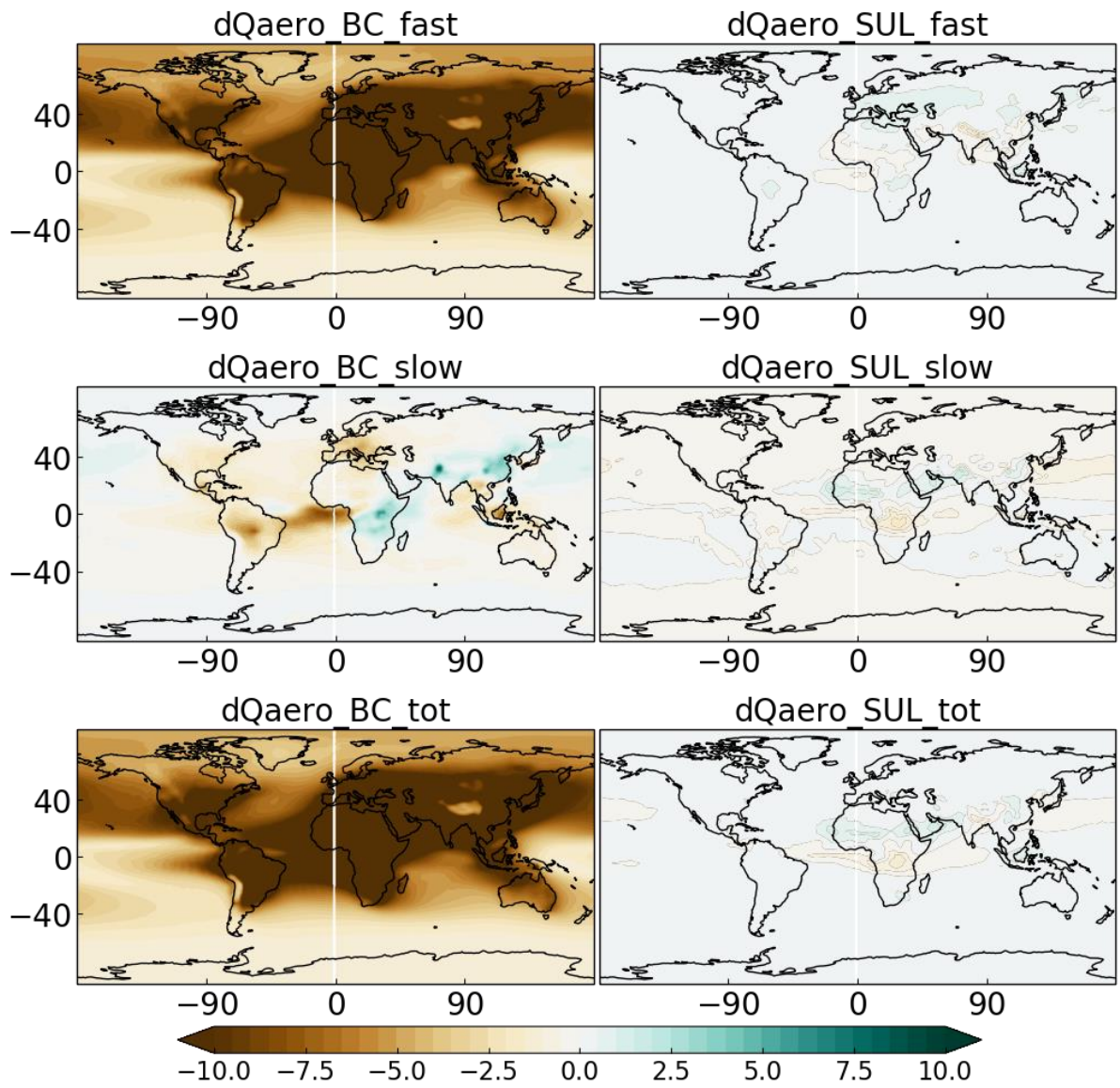


Figure S9. Same as Figure S5, but for changes in atmospheric radiative cooling from aerosols (unit: W m^{-2})

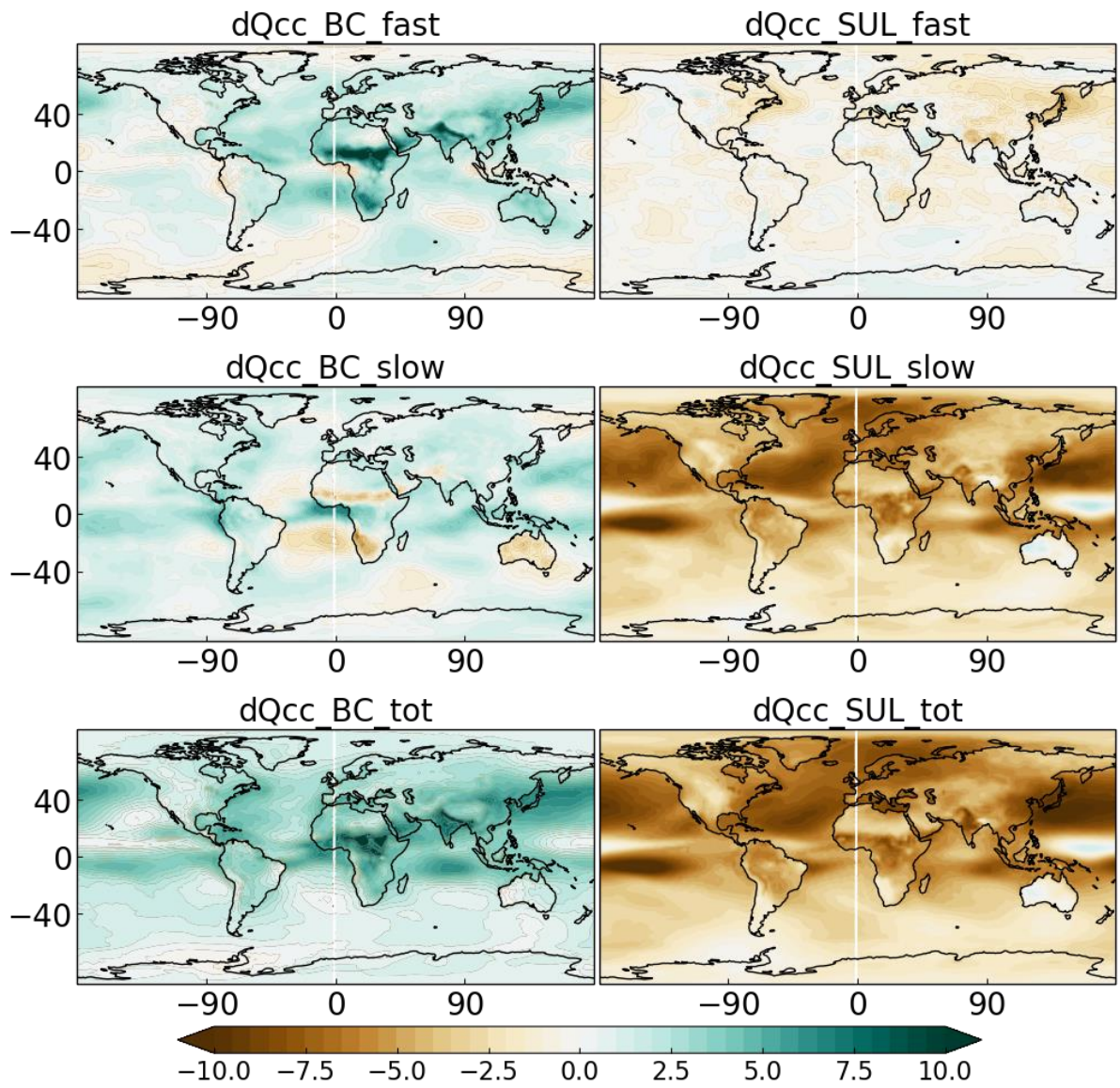


Figure S10. Same as Figure S5, but for changes in atmospheric radiative cooling from clear-clean sky (unit: $W m^{-2}$).

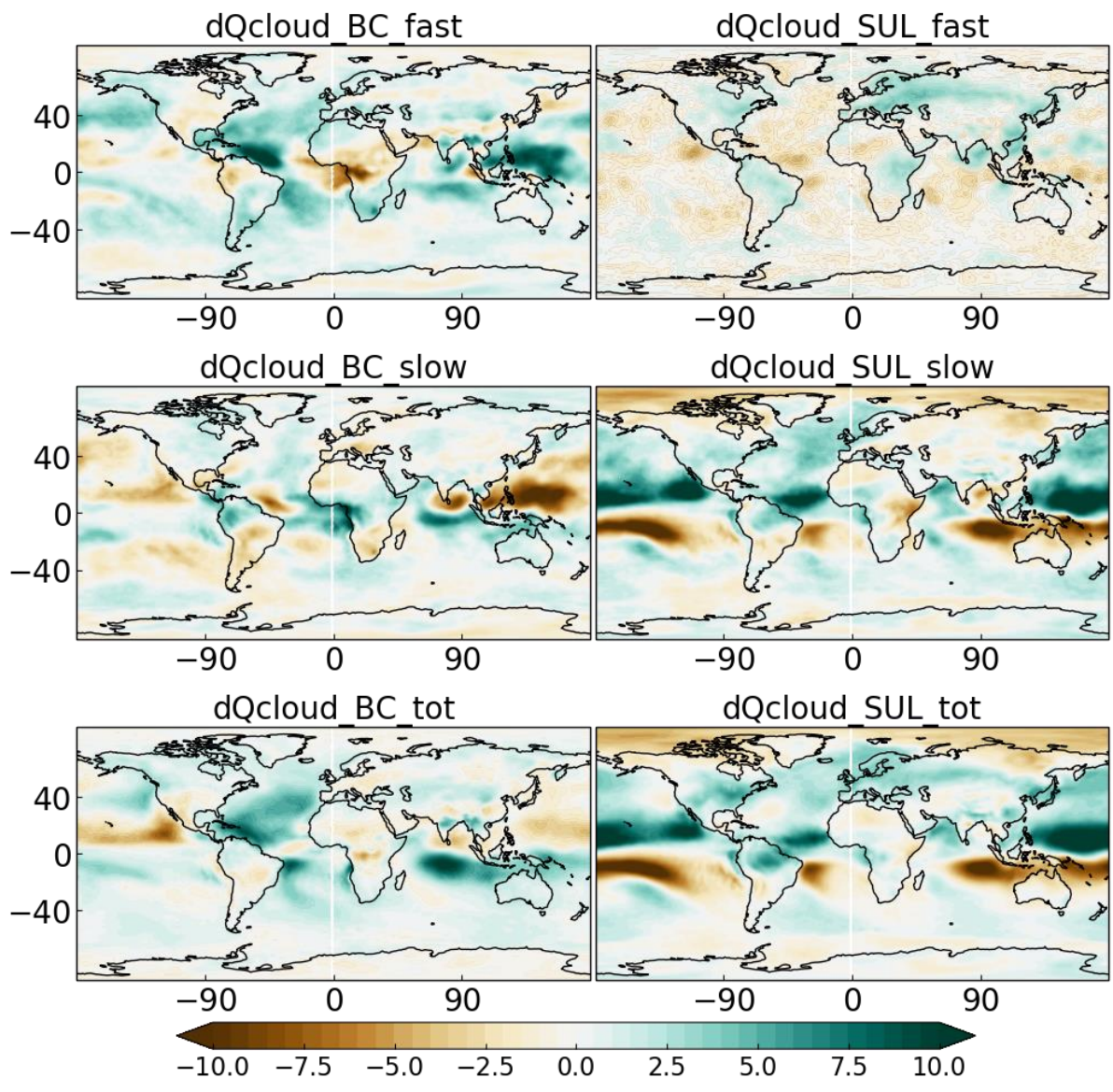


Figure S11. Same as Figure S5, but for changes in atmospheric radiative cooling from clouds (unit: W m^{-2}).

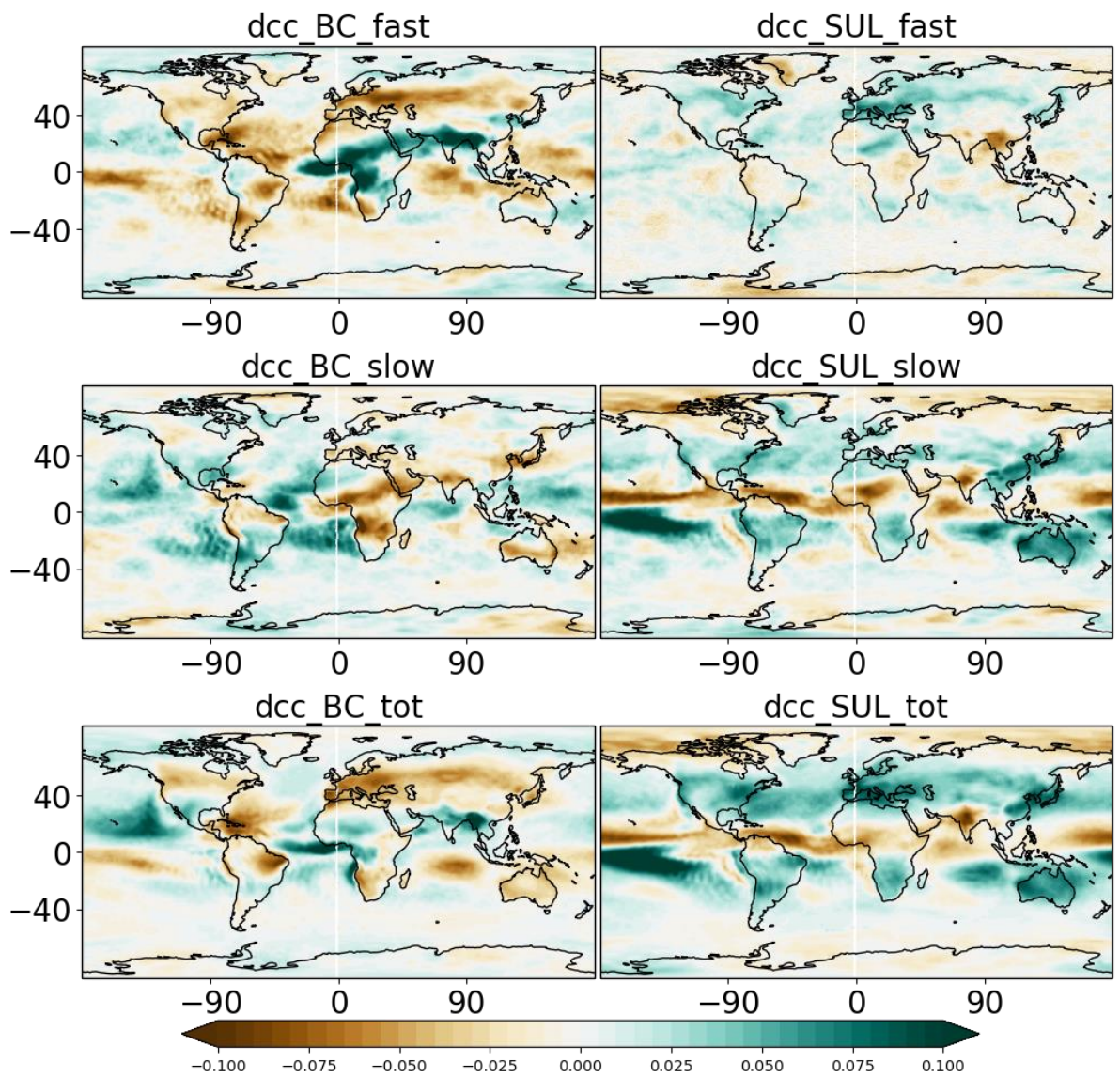


Figure S12. Same as Figure S5, but for changes in total cloud cover.

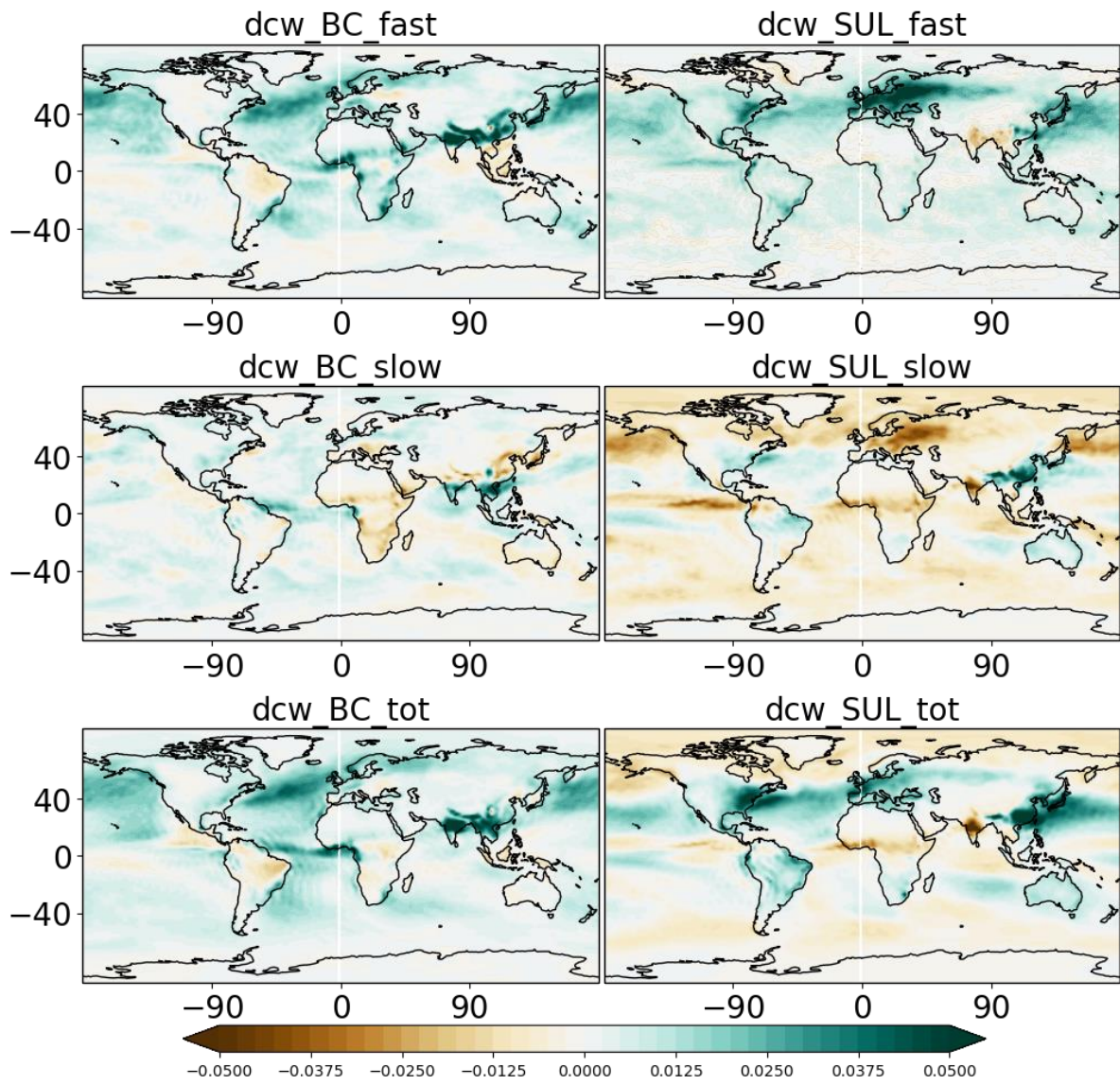


Figure S13. Same as Figure S5, but for changes in column integrated cloud water (unit: kg m^{-2}).

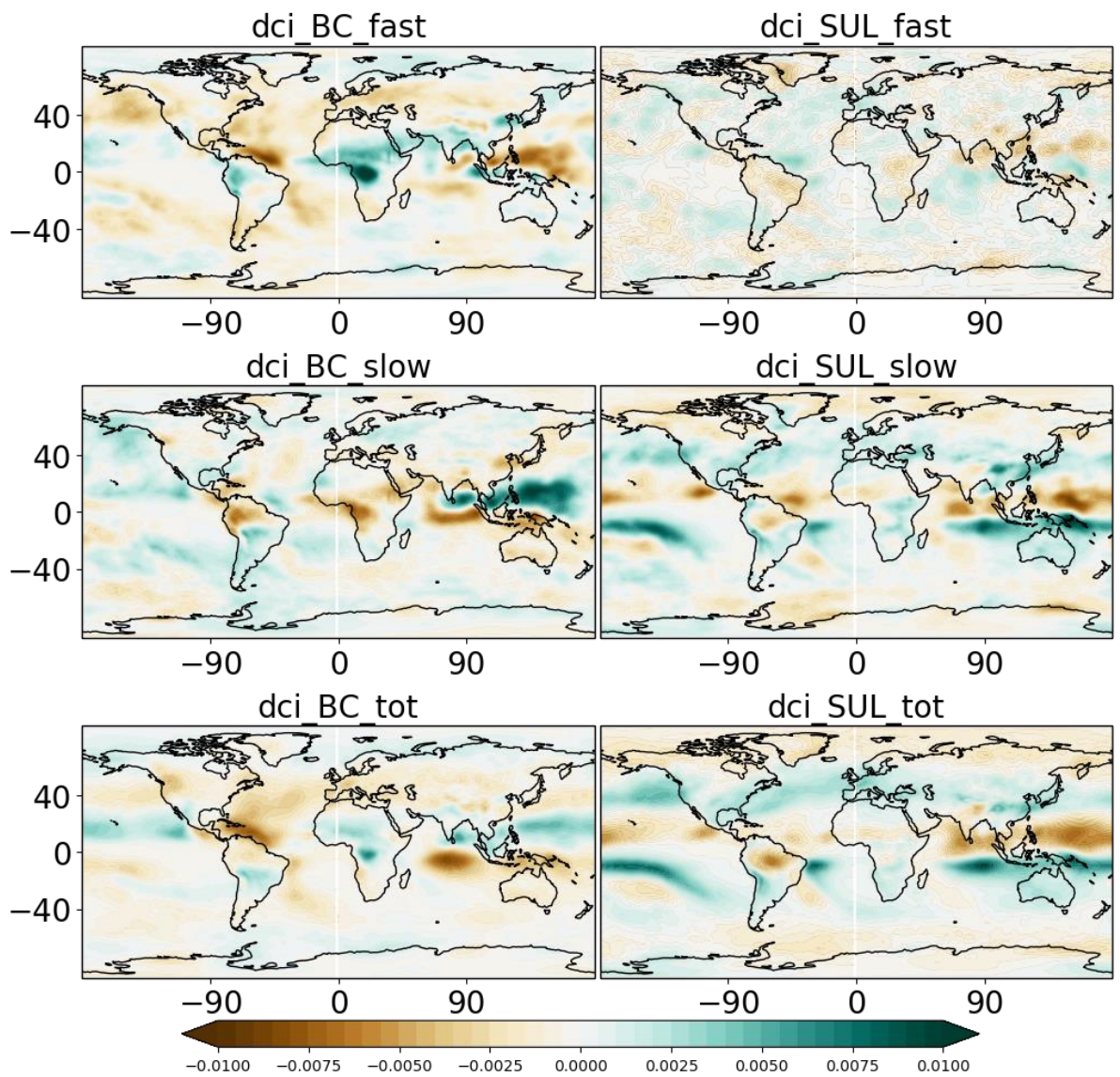


Figure S14. Same as Figure S5, but for changes in column integrated cloud ice (unit: kg m^{-2}).

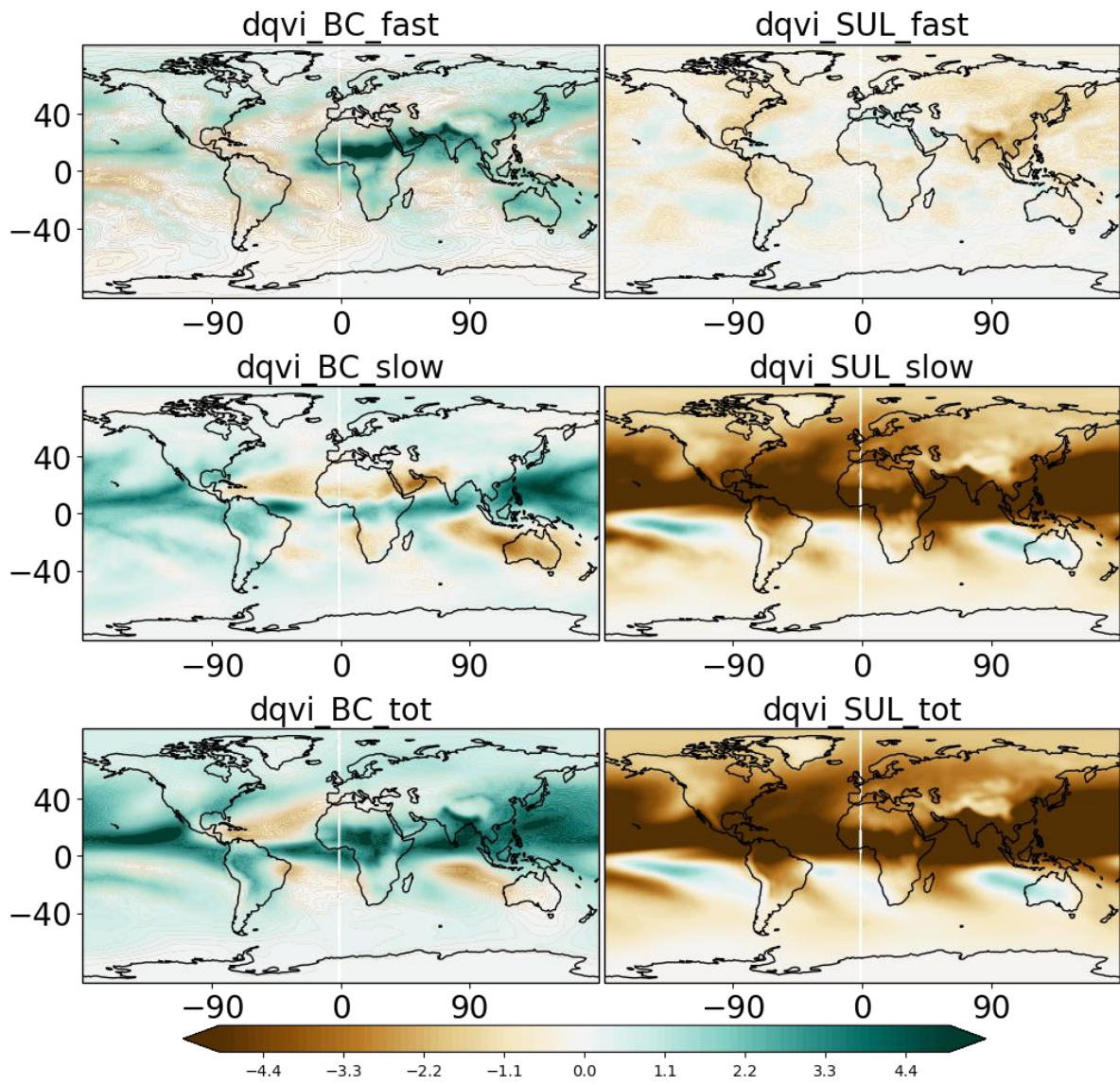


Figure S14. Same as Figure S5, but for changes in column integrated water vapour (unit: kg m^{-2}).

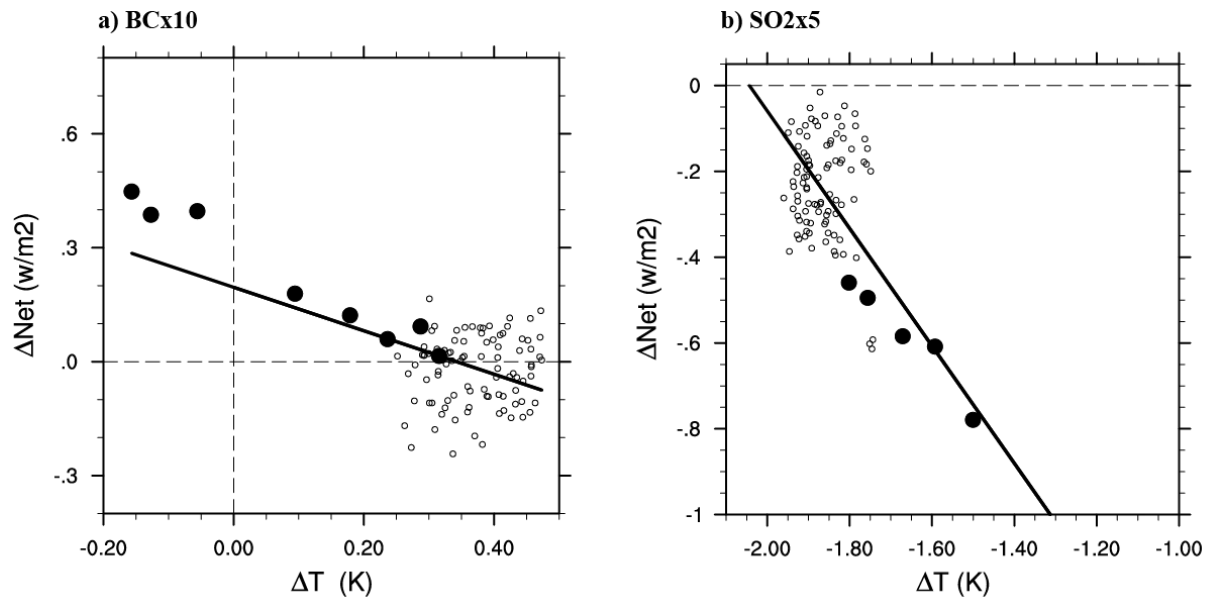


Figure S15. A Gregory-style regression between changes in surface temperature and changes in net energy flux at the top of the atmosphere, for (a)10 times black carbon and (b) 5 times sulphur dioxide perturbation experiments, respectively. Each dot represents the annual average of each individual year (100 years in total). The solid dots represent the first 8 years since the aerosol perturbations were added.